Arild Saasen[1]
Department of Energy and
Petroleum Engineering,
University of Stavanger,
4036 Stavanger, Norway
e-mail: arild.saasen@uis.no

Jan David Ytrehus
SINTEF,
S.P. Andersens vei 15 B,
7031 Trondheim, Norway
e-mail: jandavid.ytrehus@sintef.no

Bjørnar Lund
SINTEF,
S.P. Andersens vei 15 B,
7031 Trondheim, Norway
e-mail: Bjornar.lund@sintef.no

Annular Frictional Pressure Losses for Drilling Fluids

In the paper, it is demonstrated how a Herschel–Bulkley fluid model, where the parameters are selected from relevant shear rate range of the flow and are parametrically independent, can be used for pressure loss calculations. The model is found to provide adequate pressure loss predictions for axial flow in an annulus where the inner cylinder does not rotate. It is described how one can simplify a slot model approximation of the annulus pressure loss using the Herschel–Bulkley fluid model (Founargiotakis model). This simplified model gives approximately the same accuracy as does the full Founargiotakis model. It is shown that the use of such a parallel plate model gives reasonably good fit to measured data on laminar flow of oil-based drilling fluids if the viscous data are measured at relevant shear rates for the flow. Laboratory measurements indicate that the use of the simplified pressure loss model is also valid for turbulent flow. However, the predictions should be adjusted for the surface roughness in the well. [DOI: 10.1115/1.4049466]

Keywords: drilling, drilling fluid, annular pressure losses

Introduction

Annular Friction Loss. The topic of annular frictional pressure loss modeling has been a challenge in drilling engineering. To be able to select drilling fluids with proper chemical composition to avoid un-wanted interaction with the formation, it is necessary to predict the annular frictional pressure losses with a reasonable accuracy. It is important that the down hole pressures never exceed the fracturing pressure or enter pressure areas vulnerable for hole instability issues. The accessible pressure window is estimated from geological analyses and is modified by a series of formation strength tests [1] as the drilling proceeds.

The Herschel–Bulkley model includes the Bingham and power-law models by the selection of their parameters. The appearance of a non-zero yield stress makes all annular calculations complicated. A non-yielded region with constant velocity and two yield stress boundaries will be introduced, leading to a complex set of equations. Often, an iterative procedure is selected to be able to calculate the flow equations. Therefore, to simplify the calculations, it is common to use the power-law model for the fluid flow calculations. Here, the parameters can be selected to be valid for a realistic range of shear rates.

Models for annular frictional pressure losses have been treated in many drilling textbooks like for example by Ahmed and Miska [2] and Bird et al. [3]. Very seldom the models are coupled with the selection of viscosity data from measurements at the relevant shear rates. Ytrehus et al. [4] showed the importance of selecting shear stress data from the relevant shear rates in building the viscosity model for pressure loss calculations as shown in Fig. 1 for a series of experiments simulating flow inside a cased hole. By selecting the shear stress data from shear rates less than 300 s^{-1}, the accuracy of prediction was improved [4,5]. In this case, the pressure loss prediction was obtained using the Founargiotakis model [6].

Effect of Drillstring Rotation. It is earlier shown how the rotation of the inner string in an annulus can complicate the flow for example by the establishment of Taylor vortices in full scale experiments [7], field applications [8], and theoretically [9]. There are currently no analytical methods to handle such flow. The effect of

the vortices depends strongly on the fluid's composition in addition to the flow conditions. The practical way to handle these situations in offshore drilling is by "fingerprinting" during circulation, meaning comparing pressure losses directly to the pressure losses of a previously conducted similar operation at defined rotation rates.

Annular Friction Loss Predictions

Simplified Laminar Flow Model. Founargiotakis et al. [6] presented a model for laminar, transitional, and turbulent flow of Herschel–Bulkley fluids in concentric annuli, using the slot approximation.

For laminar flow, the Founargiotakis model [6] is simply a determination of the shear rate at the actual flowrate given the Herschel–Bulkley fluid model. This shear rate is used for the determination of a consistency parameter and a generalized flow index for an equivalent power-law model giving the equal shear stress at that particular shear rate. Thereafter, this consistency parameter and the associated flow index are used to calculate the pressure loss of a unidirectional flow between two parallel plates, as these two plates are applied to approximate the annulus.

The hydraulic model of Founargiotakis et al. [6] is here applied to axial flow of Herschel–Bulkley fluids in an eccentric annulus. First,
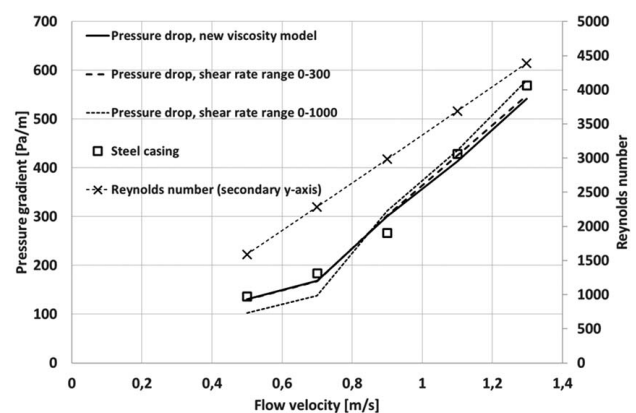
Fig. 1 Measured and calculated pressure loss of drilling fluid flow in fully eccentric simulated cased hole annulus. Modified from Ytrehus et al. [4]

we rewrite the constitutive equation for the Herschel–Bulkley model using dimensionless shear rates [5] as shown in Eq. (1):

$$\tau(\dot{\gamma}) = \tau_y + \tau_s \left(\frac{\dot{\gamma}}{\dot{\gamma}_s}\right)^n \tag{1}$$

where $\tau_s = \tau - \tau_y$ at the shear rate $\dot{\gamma} = \dot{\gamma}_s$.

Following Founargiotakis et al. [6], and by using the traditional terminology for the Herschel–Bulkley fluid where $\tau(\dot{\gamma}) = \tau_y + K(\dot{\gamma})^n$, the average velocity can be related to the annular pressure loss by Eq. (2) for laminar flow:

$$U = \left(\frac{\frac{dp}{dL}}{K}\right)^m \frac{\left(\frac{h}{2}\right)^{m+1}(1-\xi)^{m+1}(\xi+m+1)}{(m+1)(m+2)} \tag{2}$$

where the relative importance of the yield stress, ξ, is defined using Eq. (3) and dp/dL is the frictional pressure gradient. For simplicity in the equations, the inverse of the Herschel–Bulkley curvature index, m, is also used: $m = 1/n$

$$\xi = \frac{\tau_y}{\tau_w} \tag{3}$$

In Eq. (3), the wall shear stress, τ_w, is calculated for the narrow parallel plate slot model for laminar flow. The slot width is given as shown in Eq. (4):

$$h = \frac{d_o - d_i}{2} = r_o - r_i \tag{4}$$

By use of Eq. (1), the consistency, K, in Eq. (2) is removed and this equation is transferred to Eq. (5):

$$U = \left(\frac{\frac{dp}{dL}}{\tau_s}\right)^m \dot{\gamma}_s \frac{\left(\frac{h}{2}\right)^{m+1}(1-\xi)^{m+1}(\xi+m+1)}{(m+1)(m+2)} \tag{5}$$

In the slot approximation, the wall shear stress is related to the pressure loss using $(dp/dL)h = 2\tau_w$. Then, Eq. (5) is re-written as Eq. (6):

$$U = \left(\frac{\tau_w}{\tau_s}\right)^m \dot{\gamma}_s \frac{\left(\frac{h}{2}\right)(1-\xi)^{m+1}(\xi+m+1)}{(m+1)(m+2)} \tag{6}$$

This equation is solved with respect to wall shear stress for any given velocity U. The troublesome part is that the relative importance of the yield stress, ξ, is dependent on the wall shear stress, τ_w making the equation implicit in τ_w.

A possible simplification of this model is to make an estimation of the relative importance of the yield stress. The sum of the yield stress and the surplus stress will approximate the wall shear stress if the surplus stress is selected in a relevant shear rate region for the flow case. Hence, we approximate the wall shear stress as shown in Eq. (7):

$$\tau_w \approx \tau_s \sqrt[m]{\frac{2U}{h} \dot{\gamma}_s^{-1} \frac{(m+1)(m+2)}{(1-\zeta)^{m+1}(\zeta+m+1)}} \tag{7}$$

with

$$\zeta \approx \frac{\tau_y}{\tau_y + \tau_s} \tag{8}$$

Simplified Calculations Using the Power-Law Model. Equation (7) gives a prediction of the laminar frictional pressure loss. When the flow becomes turbulent, it is more convenient to express the wall shear stress in terms of a friction factor and use that one for the pressure loss calculation. It is troublesome to use

any flow curves with yield stresses in such calculations as iterative systems need to be used. Therefore, it is customary to approximate the real flow curve with a power-law function in the relevant shear rate range. In principle, a reasonable pressure loss calculation accuracy should be obtained if a power-law model is used and the power-law parameters are determined from relevant shear rates of the flow

$$\tau_{HB}(\dot{\gamma}) = \tau_y + \tau_s \dot{\Gamma}^n \tag{9}$$

$$\tau_{PL} = T_s \dot{\Gamma}^{n'} \tag{10}$$

In Eq. (9), $\dot{\Gamma}$ is the dimensionless shear rate, $\dot{\gamma}/\dot{\gamma}_s$, and in Eq. (10), $T_s = \tau_y + \tau_s$. The shear stresses τ_{HB} and τ_{PL} are by construction equal when the dimensionless shear rate is unity. When the power-law curve and the Herschel–Bulkley model curve are made using the same measurement data set, these curves must be equal also at another shear rate. It is possible to select this other shear rate by adjustment of the index n'. This is obtained by requiring that

$$n' = \frac{ln\left[\frac{\tau_y + \tau_s \dot{\Gamma}^n}{T_s}\right]}{ln\dot{\Gamma}} \tag{11}$$

where $\dot{\Gamma}$ is the dimensionless shear rate at which the value of n' shall be determined. The yield stress will be a main contributor to the shear thinning of the power-law function. Hence, n' will depend on the yield stress.

To calculate the turbulent frictional pressure loss, the friction factor concept will be used. The friction factor is defined in Eq. (12). This friction factor depends on the Reynolds number. The Reynolds number is defined as shown in Eq. (13):

$$\left|\frac{dp}{dx}\right| = \frac{2f\rho U^2}{d_o - d_i} \tag{12}$$

$$Re_{MRa} = \frac{\rho U(d_o - d_i)}{\mu_e} \tag{13}$$

In the Reynolds number, an effective, or apparent viscosity, μ_e, is used. This viscosity can only be approximated. A practical way to approximate this is by using the definition of viscosity at the wall assuming a laminar flow as shown in Eq. (14):

$$\mu_e \equiv \frac{\tau_w}{\dot{\gamma}_w} \tag{14}$$

where the wall stress is presented using Eq. (7) and the wall shear rate is given as presented in Eq. (15). This equation can be found in most textbooks on flow of complex fluids, like for example Guillot [10]

$$\dot{\gamma}_w = \frac{12U}{d_o - d_i} \frac{2n' + 1}{3n'} \tag{15}$$

By solving Eq. (16), it is now possible to calculate the friction factor, f_{turb}:

$$\frac{1}{\sqrt{f_{turb}}} = \frac{4\log_{10}[Re_{MRa}f_{turb}^{1-(n'/2)}]}{(n')^{0.75}} - \frac{0.395}{(n')^{1.2}} \tag{16}$$

The turbulent frictional pressure loss can now be calculated using Eq. (12), valid for smooth pipe. There is, however, a fairly large transition zone from laminar to fully turbulent flow. It is normal to assume two boundaries as shown in Eq. (17). These two boundaries are dependent on the shear thinning characteristics of the drilling fluid

$$Re_1 < Re_{MRa} < Re_2 \tag{17}$$

where $Re_1 = 3250 - 1150n'$ and $Re_2 = 4150 - 1150n'$ [11]. The friction factor is calculated as $24/Re_{MRa}$ for $Re_{MRa} < Re_1$, and for

$\mathrm{Re}_{MRa} > \mathrm{Re}_2$, the friction factor from Eq. (16) is used in Eq. (12). In the transition zone between Re_1 and Re_2, a linear interpolation between laminar and turbulent friction factors is often used

$$f = f_{l1} + \frac{\mathrm{Re}_{MRa} - \mathrm{Re}_1}{\mathrm{Re}_2 - \mathrm{Re}_1}(f_{t2} - f_{l1}) \qquad (18)$$

Both Eqs. (16) and (18) are dependent on the type of drilling fluid. Water-based drilling fluids with a large concentration of high molecular weight polymers have a significant different behavior than have the emulsion-based fluids. Drag reduction may occur in the water-based drilling fluids. Conventional drag reduction is not expected to appear in the flow of oil-based drilling fluids.

Corrections for Eccentricity

Haciislamoglu and Langlinais [12] and Haciislamoglu and Cartalos [13] presented models for pressure loss corrections for eccentric annuli in laminar and turbulent flow. These models are presented in Eqs. (17) and (18) for laminar flow and turbulent flow, respectively. In their work, they used the power-law consistency factor, K. This is replaced by $T_s/\dot{\gamma}_s^n$, using the method by Saasen and Ytrehus [5,14] to present the Herschel–Bulkley model with parametrically independent fluid parameters, obtained using dimensionless shear rates

$$C_l = \frac{\left(\frac{dp}{dx}\right)_{lam,e}}{\left(\frac{dp}{dx}\right)_{lam,c}} = 1 - 0.072\left(\frac{e}{n}\right)\left(\frac{T_s}{\dot{\gamma}_s^n}\right)^{0.8454}$$
$$- \frac{3}{2}(e^2\sqrt{n})\left(\frac{T_s}{\dot{\gamma}_s^n}\right)^{0.1852} + 0.96(e^3\sqrt{n})\left(\frac{T_s}{\dot{\gamma}_s^n}\right)^{0.2527} \qquad (19)$$

$$C_t = \frac{\left(\frac{dp}{dx}\right)_{lam,e}}{\left(\frac{dp}{dx}\right)_{lam,c}} = 1 - 0.048\left(\frac{e}{n}\right)\left(\frac{T_s}{\dot{\gamma}_s^n}\right)^{0.8454}$$
$$- \frac{2}{3}(e^2\sqrt{n})\left(\frac{T_s}{\dot{\gamma}_s^n}\right)^{0.1852} + 0.285(e^3\sqrt{n})\left(\frac{T_s}{\dot{\gamma}_s^n}\right)^{0.2527} \qquad (20)$$

Predictions Compared With Experiments

The shear rate where the surplus stress is measured should be at a large relevant shear rate for the flow problem. Typical shear rates are tabulated by for example Guillot [10].

For the prediction of pressure losses during flow is often sufficient to use a power-law approximation to the Herschel–Bulkley curve. In these cases, the power-law and Herschel–Bulkley flow curves should approximate each other when the shear rates are close to the surplus stress shear rate. In the sketch shown in Fig. 2, this is illustrated where a Herschel–Bulkley curve and two power-law curves given by Eqs. (9) and (10) are used if the power-law index, n', is chosen at $\dot{\Gamma} = a$, where a is either 0.5 or 0.75. If $\dot{\Gamma} = 1$ represents too high a shear rate it is expected that $a = 0.5$ would yield the most accurate results. In other cases, $a = 0.75$ is expected to give the best results.

The experimental flow loop [4] is constructed using an approximately 10 m long steel pipe with an outer annular diameter of $Do = 100$ mm simulating cased hole. The use of a stack of 20 cm long cylindrical cement inserts with similar outer annular diameter as the steel pipe was applied for tests simulating open hole drilling. A steel rod of $Di = 50.4$ mm diameter inside the wellbore represents the drill string.

Three different field applied oil-based drilling fluids were used in a set of experiments where the scope was to compare the different models with experimental data. OBM A, B, and C are labeled
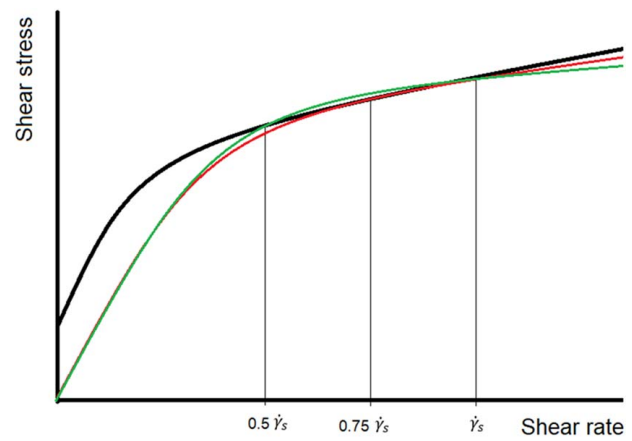
Fig. 2 Comparison between Herschel–Bulkley (Black line) and power-law curves equal to the Herschel–Bulkley curve at $\dot{\gamma}_s$ and at half that value shown by the light gray (green) line and at 75% of that value shown by the dark gray (red) line

such that the shear stress and thus the viscosity of OBM-A is less than those of OBM-B, which again is less than those of OBM-C at all the measured shear rates up to $300~\mathrm{s}^{-1}$. The resulting viscosity data are shown in Table 1 both for $a = 0.5$ and $a = 0.75$. The frictional pressure losses as function of the flowrate for these fluids are shown in Figs. 3–5 for the OBMs A, B, and C, respectively.

All the models seem to predict the same pressure loss for the flow of the thinnest drilling fluid, OBM-A, as shown in Fig. 3. At the lowest velocity of 0.5 m/s, entirely in laminar flow, the accuracy seems to be acceptable. After reaching the turbulent conditions, the accuracy seems to be acceptable for the lowest flowrate of 0.8 m/s. Thereafter, the models seem to underestimate the pressure loss. At a velocity of 0.7 m/s, the part of the flow in the widest part of the annulus is expected to be unstable, or weakly turbulent. Hence, the use of a sole laminar model underestimates this pressure loss.

By default, smooth pipe is used for the calculations in this work. For the laminar flow, this is acceptable. As the outer annulus wall was constructed from cemented cylinder segment, and the highest Reynolds numbers were in the turbulent regime, the potential effects of roughness on the pressure drop were analyzed. Since the theory for wall roughness effects on the turbulent flow of non-Newtonian fluids is not well developed, and since the roughness can vary when using the stacked cemented sections, the effect of wall roughness was evaluated simply by assuming that the effects of roughness are the same as for a Newtonian fluid at the same Reynolds number, i.e.

$$f_{HB,r} = f_{HB,s}\frac{f_{N,r}}{f_{N,s}} \qquad (21)$$

where $f_{N,r}$ and $f_{N,s}$ are the friction factors for Newtonian fluid for rough and smooth wall, respectively. Here, we represent $f_{N,r}$

Table 1 Drilling fluid viscosity parameters measured using an Anton Paar rheometer

Model fluid	Power-law $a = 0.5$		Power-law $a = 0.75$		Herschel–Bulkley		
	T_s	n	T_s	n	τ_y	τ_s	n
OBM-A	4.13	0.8225	4.13	0.8318	0.20	3.93	0.88
OBM-B	10.0	0.6524	10.0	0.6690	1.29	8.71	0.78
OBM-C	12.4	0.6680	12.4	0.6883	1.80	10.6	0.82

Note: The surplus stress shear rate is $198~\mathrm{s}^{-1}$. All stresses are in Pascals (Pa).
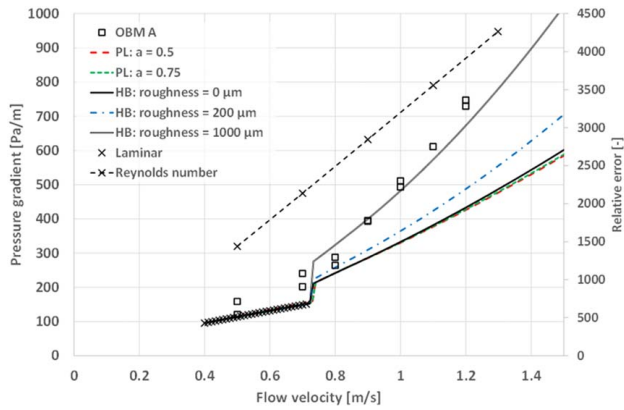
Fig. 3 Comparison of pressure gradient predictions resulting from the application of different viscosity descriptions of the same fluid measurement data for drilling fluid OBM-A in simulated open hole

using the Haaland friction factor [15]

$$\frac{1}{\sqrt{f_H}} = -3.6 \log_{10}\left[\frac{6.9}{\mathrm{Re}} + \left(\frac{k}{3.7 D_h}\right)^{1.11}\right] \tag{22}$$

where k is the absolute wall roughness.

All the smooth pipe results give nearly equal predictions. A roughness of $k = 200 \, \mu\mathrm{m}$ gives an increased predicted pressure loss. Still, this predicted pressure loss is far from the measured values, especially at higher flow velocities. Now, the junctions between the inserts will introduce some irregularities each 20 cm. These irregularities could perhaps introduce a local roughness around one millimeter or so. Therefore, a prediction with 1 mm roughness was calculated. This calculation seems to predict the pressure losses with reasonable accuracy. Hence, it is possible to conclude that the use of simplified viscosity models gives similar results as the use of full Founargiotakis model. Furthermore, the pipe surface roughness significantly affects the pressure loss in the cemented segment pipe illustrating open hole.

The laminar pressure loss calculations observed for the two more viscous drilling fluids, OBM-B (Fig. 4) and OBM-C (Fig. 5), were all reasonably good, with the simplified models presenting a slightly less accurate prediction than the more complicated. The determination shear rate of the power-law index, n, does not seem to give any significant difference. Although not of importance, the results from
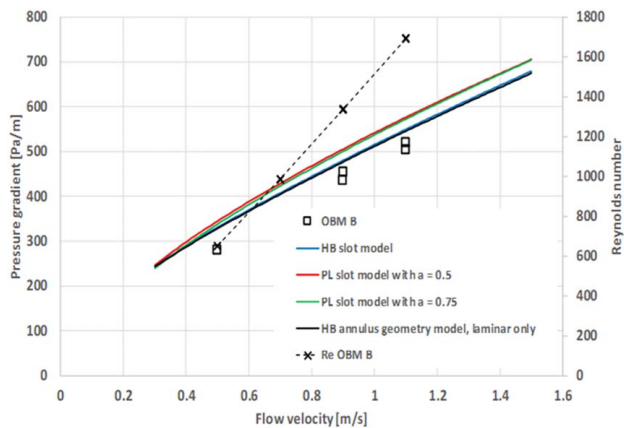
Fig. 4 Comparison of pressure gradient predictions resulting from the application of different viscosity descriptions of the same fluid measurement data for drilling fluid OBM-B in simulated open hole
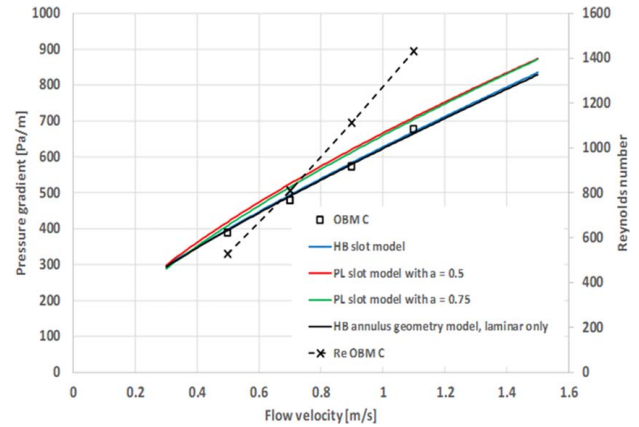
Fig. 5 Comparison of pressure gradient predictions resulting from the application of different viscosity descriptions of the same fluid measurement data for drilling fluid OBM-C in simulated open hole

selecting n at 75% of the shear rate of the surplus stress seems to be marginally better than if n was selected at 50% of that shear rate.

For laminar flow, it may be possible to use Eq. (7) directly to calculate the laminar frictional pressure loss. If this is used for OBM-A, a better correlation with the measurements is obtained than if the prediction is conducted with any of the other models. For the other two series of measurements, this correlation is not that good. For OBM-C, it is 10–15% overestimation, and for OBM-B, it is 20–25% overestimation if only Eq. (7) is used to predict the pressure losses. OBM-A is only slightly shear thinning, while both OBMS B and C are very shear thinning with OBM-B as the most shear thinning. This indicates that the degree of shear thinning complicates the pressure loss predictions. Also, the yield stress of OBM-A is smaller than that of the other two fluids.

The parallel plate slot model with pre-set values seem to be only slightly less accurate than the more complicated models with multisteps to predict laminar flow. Hence, this model may be more useful for digitalization than the other models.

Conclusion

An analysis of annular frictional pressure loss calculations with simplified models has been conducted. A pressure drop model based on parametrically independent fluid parameters is well suited to improve applications in the digitalization development currently prioritized in the drilling industry.

- The use of a parallel plate model gives reasonably good fit to measured data on laminar flow of oil-based drilling fluids if the viscous data are measured at relevant shear rates for the flow.
- The use of pressure drop estimation solely based on shear stress predicted for the anticipated shear rate of the flow will generally overestimate the predictions.
- Strong indications for an increased difficulty of predicting pressure losses if the degree of shear thinning is increased.
- Laboratory measurements indicate that the use of the simplified pressure loss model is also valid for turbulent flow. However, the predictions should be adjusted for the surface roughness in the well.

Acknowledgment

Conflict of Interest

There are no conflicts of interest.

References

[1] Økland, D., Gabrielsen, G. K., Gjerde, J., Sinke, K., and Williams, E. L., 2002, "The Importance of Extended Leak-Off Test Data for Combatting Lost Circulation," SPE/ISRM Rock Mechanics Conference, Irving, TX, Oct. 20–23, Paper No. SPE-78219-MS.

[2] Ahmed, R., and Miska, S. Z., 2009, "Advanced Wellbore Hydraulics," *Advanced Drilling and Well Technology*, B. S. Aadnoy, I. Cooper, S. Z. Miska, R. F. Mitchell, and M. L. Payne, eds., Society of Petroleum Engineers, Richardson, TX.

[3] Bird, R. B., Stewart, W. E., and Lightfoot, E. N., 1960, *Transport Phenomena*, John Wiley & Sons, New York.

[4] Ytrehus, J. D., Lund, B., Taghipour, A., Kosberg, B., Carazza, L., Gyland, K. R., and Saasen, A., 2018, "Cuttings Bed Removal in Deviated Wells," ASME 2018 37th International Conference on Ocean, Offshore and Arctic Engineering, Madrid, Spain, June 17–22, Paper No. OMAE2018-77832.

[5] Saasen, A., and Ytrehus, J. D., 2020, "Viscosity Models for Drilling Fluids—Herschel-Bulkley Parameters and Their Use," Energies, **13**(20), p. 5271.

[6] Founargiotakis, K., Kelessidis, V. C., and Maglione, R., 2008, "Laminar, Transitional and Turbulent Flow of Herschel-Bulkley Fluids in Concentric Annulus," Can. J. Chem. Eng., **86**(4), pp. 676–683.

[7] Marken, C., He, X., and Saasen, A., 1992, "The Influence of Drilling Conditions on Annular Pressure Losses," Presented at the 67th Annual Technical Conference and Exhibition, Washington D.C., Oct. 4–7, Paper No. SPE 24598.

[8] Ahmed, R., Enfis, M., Miftah-El-Kheir, H., Laget, M., and Saasen, A., 2010, "The Effect of Drillstring Rotation on Equivalent Circulation Density: Modeling and Analysis of Field Measurements," Presented at the SPE Annual Technical Conference and Exhibition Held in Florence, Italy, Sept. 19–22, Paper No. SPE 135587.

[9] Saasen, A., 2014, "Annular Frictional Pressure Losses During Drilling—Predicting the Effect of Drillstring Rotation," ASME J. Energy Resour. Technol., **136**(3), p. 034501.

[10] Guillot, D., 2006, "Rheology and Flow of Well Cement Slurries," *Well Cementing*, Ch. 4, E. Nelson, and D. Guillot, eds., Schlumberger, Sugar Land, TX.

[11] Comité des Techniciens, 1982, *Drilling Mud and Cement Slurry Rheology Manual*, Éditions Technip, Paris.

[12] Haciislamoglu, M., and Langlinais, J., 1990, "Non-Newtonian Flow in Eccentric Annuli," ASME J. Energy Resour. Technol., **112**(3), pp. 136–169.

[13] Haciislamoglu, M., and Cartalos, U., 1994, "Practical Pressure Loss Predictions in Realistic Annular Geometries," 69th SPE Annual Technical Conference and Exhibition, SPE, ed. New Orleans, Paper No. SPE 28304.

[14] Saasen, A., and Ytrehus, J. D., 2018, "Rheological Properties of Drilling Fluids—Use of Dimensionless Shear Rates in Herschel-Bulkley Models and Power-Law Models," Appl. Rheol., **28**(5), p. 54515.

[15] Haaland, S. E., 1983, "Simple and Explicit Formulas for the Friction Factor in Turbulent Pipe Flow," ASME J. Fluids Eng., **105**(1), pp. 89–90.